Desalination 547 (2023) 116240

Contents lists available at ScienceDirect

Desalination

journal homepage: www.elsevier.com/locate/desal

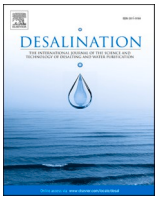

A comprehensive investigation of performance of pulsed electrodialysis for desalination of brackish water

Soraya Honarparvar [a,*,1], Rashed Al-Rashed [a,b,*,1], Amos G. Winter V. [a]

[a] Department of Mechanical Engineering, Massachusetts Institute of Technology, Cambridge, MA 02139, USA
[b] Department of Mechanical Engineering, College of Petroleum and Engineering, Kuwait University, Kuwait

HIGHLIGHTS

- Pulsed operation of electrodialysis (ED) helps suppress concentration polarization.
- Pulsed operation decreases the energy consumption and desalination rate of ED.
- Increasing the frequency and duty cycle improves the desalination rate of PED.
- Pulsed operation increases the limiting voltage and postpones water dissociation in ED.

ARTICLE INFO

Keywords:
Electrodialysis
Concentration polarization
Pulsed operation
Pulsed electrodialysis
Specific energy consumption
Desalination rate

ABSTRACT

Pulsing the electric field is an operational strategy for suppressing concentration polarization (CP) in electrodialysis (ED). In this study, the effects of pulsing parameters on the desalination performance of ED were investigated. Experimental analyses were performed at sub-limiting and limiting regimes for frequencies of 0.5–100 Hz and duty cycles of 20–80 %. A 1-D transient model was developed to calculate the concentration profiles inside the cell. The results indicated that under the same input voltage, the cycle-averaged current density of the pulsed ED (PED) increased at higher frequencies and duty cycles while always remaining below the current density of conventional ED (CED). The energy savings gained from suppressing CP compensated for the inefficiencies introduced due to the longer desalination time, resulting in approximately similar specific energy consumption (SEC) compared to CED. Pulsed operation increased the limiting voltage, allowing for higher input voltages without intensifying water dissociation. However, increasing the pulsing voltage led to a higher SEC and reduced the effectiveness of the approach for suppressing CP. To enhance the viability of PED, pulsing parameters should be tuned according to the desalination objectives. This study provides the required insights for developing a generalizable optimization approach for PED.

1. Introduction

Climate change, population growth, and increased consumption are exacerbating the global water scarcity issue. Enabling the usage of saline water supplies is a key method for reducing the gap between limited resources and growing demands. Brackish water is an attractive alternative to freshwater due to its low salinity and widespread availability in many water-scarce areas. According to the report prepared by the US Geological Survey [1], the majority of brackish groundwaters in the USA have salinity ten times lower than seawater. To meet drinking water standards [2], the total dissolved solid of brackish water should be further reduced to below 500 mg/L. Electrodialysis (ED) is an electromembrane desalination technique that is energy-efficient for the treatment of brackish water with salinity <3000 mg/L [3,4].

In ED, an electric field is utilized to drive ions through anion and cation exchange membranes (AEM and CEM, respectively), alternately placed between two electrodes (Fig. 1). The selective transport of counterions through ion exchange membranes (IEMs) results in the net transfer of ions from one channel to adjacent compartments, forming diluate and concentrate streams at the cell outlet. In ED, the higher transport number of ions inside IEMs results in the formation of concentration gradients in the vicinity of the membranes. This phenomenon, which is termed concentration polarization (CP), adversely affects

* Corresponding authors.
E-mail addresses: shonar@mit.edu (S. Honarparvar), alrashed@mit.edu (R. Al-Rashed).
[1] Co-first-authors – authors with the same contributions.

https://doi.org/10.1016/j.desal.2022.116240
Received 10 July 2022; Received in revised form 9 October 2022; Accepted 4 November 2022
Available online 18 November 2022

Nomenclature

AEM	Anion exchange membrane
BL	Boundary layer
CBL	Concentrate boundary layer
CED	Conventional electrodialysis
CEM	Cation exchange membrane
CP	Concentration polarization
DBL	Diluate boundary layer
DR	Desalination rate
ED	Electrodialysis
IEMs	Ion exchange membranes
MCDI	Membrane capacitive deionization
PED	Pulsed electrodialysis
SEC	Specific energy consumption
SD	Swelling degree

the desalination performance of the process. Under severe CP, ionic concentrations at the membrane/solution interface in the diluate boundary layers (DBLs) approach zero, leading to the formation of the "limiting condition" in the ED system. Water dissociation and pH changes increase beyond the limiting voltage. CP also increases the ions' supersaturation degree within the concentrate boundary layers (CBLs), intensifying salt formation and attachment to membrane surfaces. Concentration depletion in DBLs and membrane fouling/scaling increase the electrical resistance of the system, reducing the energy efficiency of the process. Hence, mitigating CP can substantially improve the lifetime and efficiency of ED.

Pulsed operation is a strategy to suppress CP and potentially prevent water dissociation, membrane clogging, and power inefficiency. Pulsed ED (PED) utilizes a non-stationary electric field that consists of pulsing periods (t_{on}) with an imposed voltage followed by pausing lapses (t_{off}) with zero current. During the pulses, CP forms in the boundary layers (BLs) (Fig. 2a) while during the pauses, ions diffuse from the bulk stream toward the membrane interface in the DBL and away from the interface toward the bulk solution in the CBL (Fig. 2b). The relaxation time provided during pauses allows for the partial or full return of boundary concentrations back to their bulk values (Fig. 2c). The effectiveness of the pulsed operation for mitigating CP heavily relies on the appropriate selection of pulsing voltage (U_{pulse}) and temporal parameters, which include the duty cycle (α) and frequency (f) as defined in Eqs. (1) and (2).

$$\text{Duty cycle } (\alpha) = \frac{t_{on}}{t_{on} + t_{off}} \tag{1}$$

$$\text{Frequency } (f) = \frac{1}{t_{on} + t_{off}} \tag{2}$$

In prior studies [5–22], PED was experimentally investigated under various pulsing frequencies (0.02–200 Hz) and duty cycles (20–90 %) at sub-limiting to extreme over-limiting conditions for a variety of water compositions ranging from simple NaCl solutions to dairy wastewater. In the over-limiting regime, greater electro-convective vortices were formed in PED due to the non-uniform electric field, increasing the desalination rate (DR) of the process compared to conventional ED (CED) [13,23]. At sub-limiting conditions with feedwater sustaining a high scaling propensity, pulsing reduced membrane clogging, which improved the DR of PED [6–8,10,18–21,24–26]. However, in the absence of scale-precipitating components, the DR of PED was reported to be lower than that of CED [11,17,22]. Conflicting results were reported regarding the impacts of the pulsed operation on pH changes, where PED demonstrated reduced [10,17,26], intensified [5,6], or equal [22] pH variations as those of the equivalent CED. Overall, pulsed operation under certain conditions enhanced the DR [5,12,13,19–21,23], decreased pH changes [17,22], reduced specific energy consumption (SEC) [20,22], and reduced/removed membrane fouling and scaling [6–8,10,15,16,19–22,24–28] in ED.

Ion transport in PED has been theoretically investigated in multiple studies as well [12,23,29]. Mishchuk et al. [23] developed a 1-D transient model for the DBL of ED using the Nernst-Planck (NP) equation and the electroneutrality assumption. Co-ion transport through the

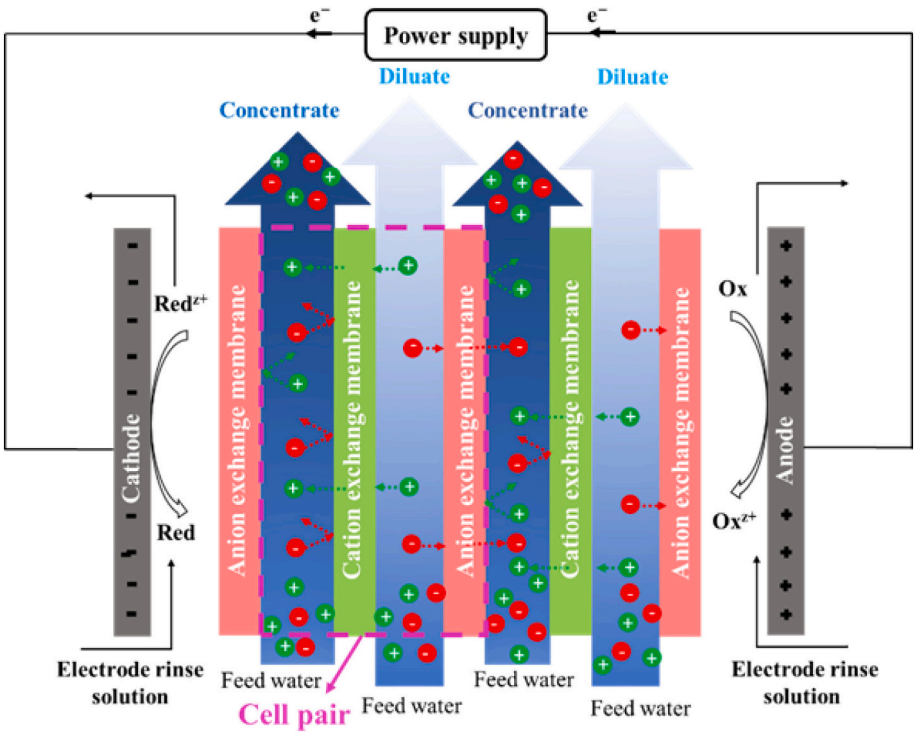

Fig. 1. A schematic diagram of an electrodialysis stack. An ED stack consists of repeating unit cells that contain an AEM, a CEM, a diluate, and a concentrate channel.

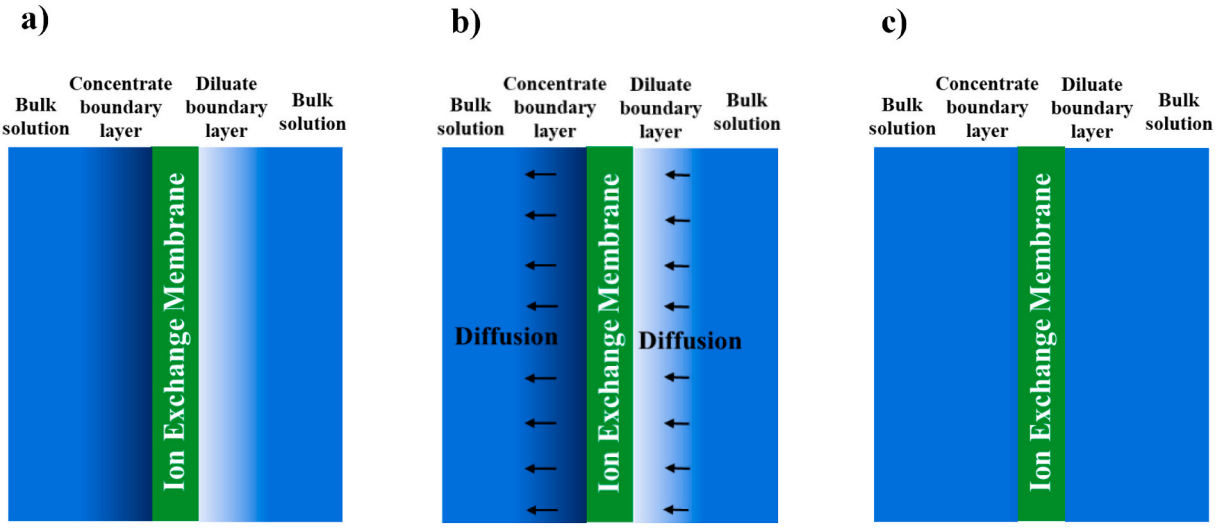

Fig. 2. a) Formation of concentration polarization at the end of the pulsing period, b) ionic diffusion from/toward the bulk solution to/from the boundary layers at the beginning of the pausing period, c) formation of uniform concentration profile in the vicinity of the membrane at the end of pausing time.

membranes was neglected and Donnan equilibrium was assumed at the membrane/solution interface. According to their results, the potentiostatic mode, where potential was fixed and the current was allowed to vary, was favored for pulsed operation due to its relatively small transition period to a stationary polarized state. Sistat et al. [12] expanded the 1-D transient model to a five-layer domain which included a CEM and two adjacent diluate and concentrate boundary and bulk layers. The concentration dependence of the NaCl diffusion coefficient was modeled using the Nernst-Hartley equation. The CEM was assumed to be a microheterogeneous system made of a nanoporous gel phase containing the membrane fixed charges and mobile counterions which existed at Donnan equilibrium with the electroneutral solutions that filled the interconnected spaces. The developed model was employed to investigate the evolutions of concentration and potential profiles during a pulsing cycle in PED operated at the voltage of $U_{pulse} = U_{CED}/\alpha$. The authors did not account for the possibility of reaching over-limiting conditions at such high pulsing voltage, under which the considered Donnan equilibrium and electroneutrality assumptions could be violated. Marti-Calatayud et al. [29] also developed a 5-layer 1-D transient model for PED operated at galvanostatic mode using the NP equation with the electroneutrality assumption. The CEM was considered to be a dense phase with fixed transport numbers for Na^+ and Cl^-. The model was employed to evaluate the effects of frequency and duty cycle on the concentration profile, current density, SEC, and DR of PED.

Prior experimental evaluation of PED implemented time-consuming trial-and-error approaches for the selection of pulsing parameters and failed to provide a thorough understanding of their impacts to enable the development of a systematic approach to optimize PED. Even the studies that merely focused on simple water chemistries (NaCl solutions) [12,13,17,23,29,30] reported non-comprehensive results regarding the performance of PED relative to CED, making it cumbersome to derive any meaningful conclusions. In studies focused on the theoretical investigation of PED, the modeling domains were limited to a narrow segment of the ED cell. These models did not account for differences in diffusion coefficients of Na^+ and Cl^- in the solution and neglected the effects of tortuosity and porosity of the spacers mesh on ions mobilities inside channels. Taking into account that diffusion is the main transport mechanism during the pausing period, an accurate estimation of ionic diffusion coefficients provides a more realistic representation of the time required for concentration recovery in PED. In the existing literature, minimal details were reported regarding the impact of pulsing on the limiting condition that controls the extent of pH variations in the ED.

In this study, we developed a 1-D transient model to calculate ion transport and concentration distributions in an ED cell and constructed a bench-scale PED unit to experimentally evaluate the system at frequencies of 0.5–100 Hz and duty cycles of 20–80 %. Simple NaCl solutions (2000 to 250 mg/L) were used as the feed water to determine the effects of pulsing parameters in the absence of scale-precipitating components. The insights gained by the NaCl solution will be used in our future study to identify the effects raised due to the scale formation when using the synthesized brackish water with a high scaling propensity. Here, we aimed to (i) determine the impacts of pulsing temporal parameters on the limiting condition of ED to evaluate the possibility of imposing higher voltage during the on-period without intensifying pH changes; (ii) identify the maximum threshold for pulsing frequency beyond which its impact on current density becomes negligible; (iii) determine the effects of duty cycle on current density; (iv) evaluate the effects of duty cycle, frequency, and pulsing voltage on SEC and DR of PED; and (v) identify the concentration distributions under various pulsing conditions to evaluate the effectiveness of the approach for moderating CP. Developing a comprehensive parametric understanding of PED is an essential step in assessing the effectiveness, energy efficiency, and viability of the pulsed operation as a scale mitigation strategy for ED. Such understanding will further provide the guideline required for developing a generalizable approach for optimizing the process according to the feedwater composition, leveraging the scale-mitigation benefits of the pulsed operation while maintaining a high production rate and low SEC.

2. Modeling framework

Theoretical modeling of an ED cell enables calculating the evolution of concentration and potential profiles in the system, facilitating the evaluation of the effects of different pulsing parameters on reducing CP. An ED cell is the repeating unit of the stack and contains an AEM, a CEM, a diluate channel, and a concentrate channel, with flow spacers located between membranes to separate them and promote mixing. A transient 1-D ion transport model was developed for an ED cell using fundamental equations applicable to electrochemical systems. Due to the analogous potential drops and ion transport across each repeating cell, a model developed for a single unit can be extended to the entire ED stack. Fig. 3 represents the modeling domains, which include a CEM, an AEM, DBLs, CBLs, and diluate and concentrate bulk solutions. To represent the potential drops imposed across a cell, a hypothetical cathode and anode are placed on the left- and right-most boundaries, respectively. The developed framework with the assumptions defined below is solved

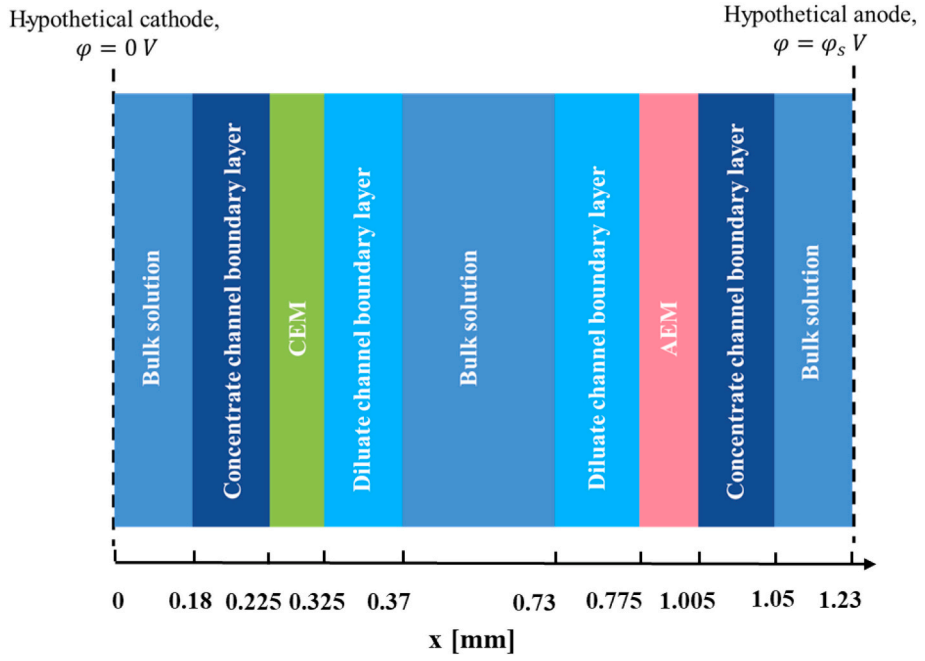

Fig. 3. A schematic diagram of an ED cell containing all the modeling domains.

numerically using the finite difference method with the linear discretization of the domains (finer mesh size in BLs).

2.1. Modeling assumptions and input parameters

Due to the short residence time and presence of the spacer mesh in channels, the concentration profile in the bulk solution is assumed to remain uniform and constant. The no-slip boundary at the membrane-solution interface results in the formation of stagnant BLs with varying concentrations. The thickness of BL depends on the hydrodynamics of the system and can reach up to hundreds of micrometers [31]. Here, BLs thicknesses are estimated to be 10 % of the channel width. Feedwater is assumed to contain NaCl which fully dissociates to Na^+ and Cl^- in the solution. The non-ideal solution behavior effects are considered to be negligible within the concentration range of this study [32]. In the sub-limiting regime, which is the focus of the current effort, water dissociation is minor. The model does not account for osmosis and electro-osmosis transport of water through the membranes and convective fluxes in the x-direction are neglected. Channel width is assigned according to the thickness of the spacer used in the experimental stack (ED 64004, PCCell, Germany). Membrane properties used in the model including thickness, swelling degree (SD), the density of the polymer, and fixed charges concentrations are obtained from experimental measurements reported by Kingsbury et al. [33] for the PCCell PC-SA (AEM) and PCCell PC-SK (CEM) membranes used in the experimental portion of this study (PCCell GmbH, Heusweiler, Germany). A summary of model input parameters is provided in Table 1.

2.2. Modeling ion transport in channels

The molar balance equation for species i in channels (bulk and boundary layers) is described as

$$\frac{dc_i(x,t)}{dt} = \nabla . N_i(x,t), \tag{3}$$

where c_i and N_i denote the concentration and molar flux of species i in solution, respectively. In the absence of convection, diffusion and electromigration are the main ion transport mechanisms in an ED cell. The Nernst-Planck equation, as presented in Eq. (4), is used to calculate the ionic fluxes within channels.

Table 1
Model input parameters.

Parameter	Value	Unit
Channel thickness, H	0.45	mm
Boundary layers thicknesses, H_{BL}	0.045	mm
CEM thickness, H_{CEM}	0.1	mm
AEM thickness, H_{AEM}	0.23	mm
Feedwater concentration, c_{feed}	2000–250	mg/l
Temperature, T	298.15	K
Na^+ Diffusion coefficient in water, D_{Na}	1.33×10^{-9}	m^2/s
Cl^- Diffusion coefficient in water, D_{Cl}	2.03×10^{-9}	m^2/s
CEM fixed charges concentration, $c_{f,CEM}$	3400	mol/m^3 absorbed H_2O
AEM fixed charges concentration, $c_{f,AEM}$	5900	mol/m^3 absorbed H_2O
Swelling degree of CEM, SD_{CEM}	0.37 [33]	g H_2O/g dry polymer
Swelling degree of AEM, SD_{AEM}	0.29 [33]	g H_2O/g dry polymer
Density of water, ρ_w	1	g/cm^3
Density of polymer, ρ_P	1.15 [33]	g/cm^3

$$N_i(x,t) = -D_i\frac{dc_i(x,t)}{dx} - \frac{D_{i,eff}}{RT}Fz_ic_i(x,t)\frac{d\varphi(x,t)}{dx} \tag{4}$$

Here, D_i and $D_{i,eff}$ are, respectively, the diffusion coefficient and effective diffusion coefficient of species i in channels; R denotes the universal gas constant (8.314 J/mol·k); T is the temperature of the system; F is the Faraday number (9.6×10^4 C/mol); z_i is the charge number of species i; and φ is the potential of the solution. The porosity (ε) and tortuosity (τ) of the spacer mesh in channels affect ion mobility in the solution [34]. Hence, effective diffusion coefficients, defined as Eq. (5), are employed for electromigration fluxes to take these effects into account. For diffusion fluxes, the higher dispersion due to the enhanced mixing in spacer-filled channels compensates for the porosity and tortuosity effects. Therefore, the infinite dilution diffusion coefficients are used to calculate diffusion fluxes. An experimentally identified ε/τ of 0.314 reported by Patel et al. [4] is employed in this study.

$$D_{i,eff} = \frac{\varepsilon}{\tau}D_i \tag{5}$$

Substituting Eq. (4). into Eq. (3). results in Eq. (6).

$$\frac{dc_i(x,t)}{dt} = D_i\frac{d^2c_i(x,t)}{dx^2} + \frac{D_{i,eff}}{RT}Fz_i\frac{dc_i(x,t)}{dx}\frac{d\varphi(x,t)}{dx} + \frac{D_{i,eff}}{RT}Fz_ic_i(x,t)\frac{d^2\varphi(x,t)}{dx^2} \quad (6)$$

For a system including N species, Eq. (6). leads to a system of N equations and $N + 1$ unknowns which include the concentration of N species and the electric field. The extra equation required to solve the system of equations is provided with the electroneutrality assumption as described in Eq. (7). At sub-limiting conditions, electroneutrality holds everywhere in an ED cell. At above-limiting conditions, charge separation may occur, violating the electroneutrality assumption. Under such conditions, the Poisson equation will be employed in lieu of the electroneutrality assumption to calculate the potential field in the solution [35].

$$\sum_i z_ic_i(x,t) = 0 \quad (7)$$

According to Ohm's law, the current density in the cell during the on-times is calculated as

$$I_{on} = F\sum_i z_iN_i(x,t_{on}) \quad (8)$$

Current density during the pausing periods, I_{off}, is set to zero.

$$I_{off} = F\sum_i z_iN_i\left(x,t_{off}\right) = 0 \quad (9)$$

2.3. Modeling ion transport in membranes

Similar to the solution in channels, total ionic fluxes in IEMs are calculated using the Nernst-Planck equation.

$$N_{i,m}(x,t) = -D_{i,m}\frac{dc_{i,m}(x,t)}{dx} - \frac{D_{i,m}}{RT}Fz_ic_{i,m}(x,t)\frac{d\varphi_m(x,t)}{dx} \quad (10)$$

Here, $N_{i,m}$ refers to total fluxes of ions inside IEMs; $c_{i,m}$ is the concentration of species i in membranes; $D_{i,m}$ is the diffusion coefficient of species i in membranes; and φ_m denotes the potential of IEMs. The tortuosity effects raised due to the polymeric chain of membranes change the diffusion and mobility of ions inside membranes relative to the solution. According to Mackie and Mears [36] model (Eq. (11)) the diffusion coefficient of species i in the membrane is calculated from its diffusion coefficient in the solution using the membranes' volume fraction of water, ϕ_w.

$$\frac{D_{i,m}}{D_i} = \left(\frac{\varnothing_w}{2-\varnothing_w}\right)^2 \quad (11)$$

ϕ_w is calculated using the SD of membranes, density of the polymer, ρ_p, and density of water, ρ_w [33].

$$\varnothing_w = \frac{SD}{SD + \frac{\rho_w}{\rho_p}} \quad (12)$$

Employing molar balance inside IEMs leads to Eq. (13). which combined with the electroneutrality assumption described as Eq. (14). are solved to calculate the concentration and potential distributions in membranes. Electroneutrality in IEMs accounts for membrane fixed charge concentrations ($c_{f,m}$) in addition to concentrations of free ions, $c_{Na+,m}$ and $c_{Cl-,m}$. The charge number of fixed charges ($z_{f,m}$) is −1 in the CEM and 1 in the AEM.

$$\frac{dc_{i,m}(x,t)}{dt} = D_{i,m}\frac{d^2c_{i,m}(x,t)}{dx^2} + \frac{D_{i,m}}{RT}Fz_i\frac{dc_{i,m}(x,t)}{dx}\frac{d\varphi_m(x,t)}{dx} + \frac{D_{i,m}}{RT}Fz_ic_{i,m}(x,t)\frac{d^2\varphi_m(x,t)}{dx^2} \quad (13)$$

$$\sum_i z_ic_{i,m}(x,t) + z_{f,m}c_{f,m} = 0 \quad (14)$$

During pausing periods, the current density in membranes ($I_{m,off}$) is set to zero similar to that in the solution.

2.4. Boundary and initial conditions

A number of boundary and initial conditions are employed to solve the system of equations to calculate concentration and potential distributions in the cell. Ionic concentrations in the bulk solution remain the same as the feedwater concentrations, c_{feed}, due to the well-mixed condition and short residence time in channels.

$$c_{Na}(x,t) = c_{Na}(x,t) = c_{feed} \quad (15)$$

There is no local accumulation of charge in the cell. Hence, continuity of ionic fluxes and current density (Eqs. (16) and (17), respectively) hold at the membrane-solution interface.

$$N_i = N_{i,m} \quad (16)$$

$$I_{on} = I_{on,m} \quad (17)$$

Donnan equilibrium (Eq. (18)) is assumed to exist at the membrane-solution interface. This approximation is valid at the sub-limiting condition where charge separation is negligible [35].

$$\varphi_m - \varphi = \frac{RT}{Fz_i}ln\left(\frac{c_i}{c_{i,m}}\right) \quad (18)$$

During the on-time, potentials at the left and right most boundaries are defined as

$$\varphi(0,t) = 0 \quad (19)$$

and

$$\varphi(H_{cell},t_{on}) = \varphi_s, \quad (20)$$

where H_{cell} is the thickness of the cell calculated as

$$H_{cell} = 2H + H_{CEM} + H_{AEM} \quad (21)$$

Here, H, H_{CEM}, and H_{AEM} denote the channel width, the thickness of the CEM, and the thickness of the AEM, respectively. During the pausing periods, the potential at H_{cell} is calculated from

$$I_{off}\left(H_{cell},t_{off}\right) = 0 \quad (22)$$

3. Experimental materials and methods

3.1. Material and experimental setup

A bench-scale experimental setup, shown in Fig. 4a, was designed and assembled to investigate the performance of ED under various operational conditions. The schematic diagram presented in Fig. 4b indicates the most important system components, including the hydraulic loop and associated sensors. The system consisted of two hydraulically isolated loops, one for each of the diluate and concentrate streams. A positive displacement peristaltic pump (EW-07522, Cole-Parmer, USA) was used to ensure a consistent flowrate throughout the experiments. 20 μm filters were located immediately downstream of the pump to remove colloidal particles from the feedwater. A pair of pressure accumulators (SFAT-075, SEAFLO, China) were used to reduce pressure fluctuations across the stack. An ED unit (ED-64002, PCCell, Germany) containing three cell pairs made of homogeneous PCCell PC-SA and PCCell PC-SK (CEM) membranes with an active area of 64 cm^2 was used in the setup. Membranes' physicochemical properties were provided by the manufacturer and experimentally identified in the study done by Kingsbury et al. [33]. The thickness of the flow spacers used within the ED stack was 0.45 mm, and the flow path width and length were both 80 mm.

NaCl (≥99.5 % purity AR grade, VWR, USA) was mixed with distilled water (conductivity ≤ 5 μS/cm) to prepare feed solutions with salinities of 250 and 2000 mg/L. The electrode rinse solution was prepared by mixing Na_2SO_4 (≥99.0 % purity ACS grade, VWR, USA) with distilled

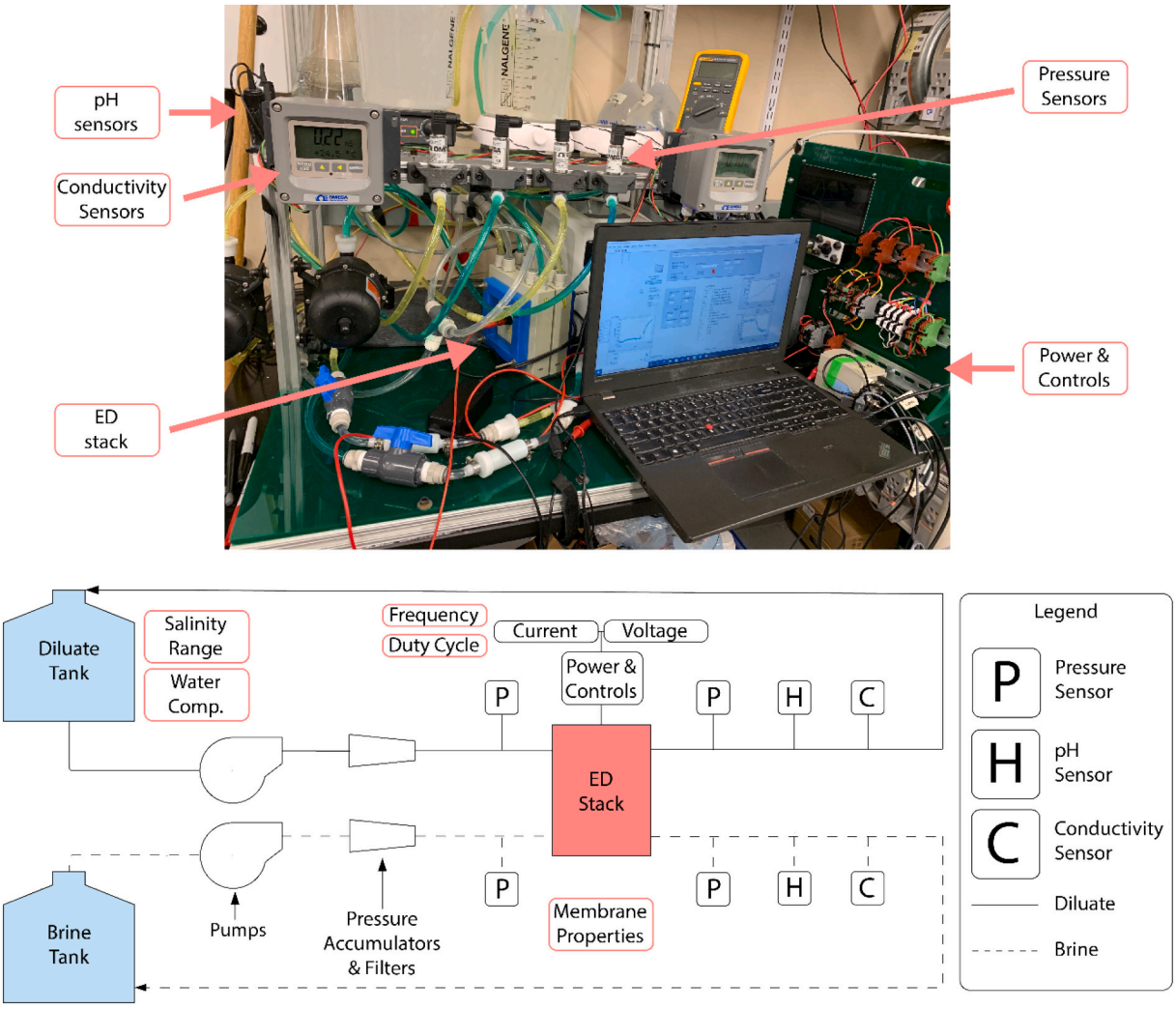

Fig. 4. a) An image of the constructed bench-scale PED experimental set-up, b) a schematic diagram of the hydraulic components of the experimental set-up.

water to produce a 0.2 mol/L solution which was recirculated through the electrode compartment at a flowrate of 150 L/h using a diaphragm pump (BYT-7A108, Bayite, China). All the experiments were conducted at room temperature (~25 °C). System monitoring and data gathering were performed through an array of sensors in the experimental setup. Pressure sensors (PX-319, Omega, USA) were located before and after the stack, allowing for the measurement of pressure drops across both streams. Additionally, conductivity (CDE-45P, Omega, USA) and pH (PHE-5311, Omega, USA) sensors were placed downstream of the stack to determine the progress of the batch and detect water dissociation, respectively.

System power delivery, control, and data acquisition were all managed by a control panel, as shown at the right of Fig. 4a. Control of the voltage and current sent to the stack, along with voltage data collection, were performed by a buck converter (DPS5005, Ruideng, China) connected to a 48 V power supply. A MOSFET (RFP30N06LE, Fairchild Semiconductor, USA) and a current sensor (ACS723, Allegro, USA), placed in series with the ED stack, allowed for high-frequency current control and measurement. Data acquisition devices (NI-DAQ 9205, 9208, and 9375, National Instruments, USA) interfaced with the system's sensors and facilitated system monitoring. LabVIEW was employed to control input parameters including stack voltage, pulsing frequency, and duty cycle as well as collect data during experiments for diagnostics and analysis purposes.

3.2. *Limiting current measurements*

In general, ED is operated at 70–90 % of its limiting voltage to avoid water dissociation and pH changes [37]. Limiting voltage and current density were identified for CED and PED by measuring the steady-state current density while increasing the input voltage from 3 to 24 V at 0.5 V intervals every 60 s. All measurements were taken while recirculating a 2 L solution of 250 mg/L NaCl with a flowrate of 9 L/h (linear channel velocity of 4.5 cm/s). The steady-state current density was determined by averaging the current density within the last 5 s of operation at each voltage-increasing step. The limiting condition of PED was measured at frequencies of 0.5 Hz, 10 Hz, 50 Hz, and 100 Hz, and duty cycles of 20 %, 50 %, and 80 %. The voltammetry (current-voltage) curve was plotted using the measured steady-state current density at each step. In general, a voltammetry curve for an ED system contains a sub-limiting region with a linear increase in current density followed by a region where the current-voltage slope sharply decreases, which indicates the onset of the limiting condition. For each experiment, the limiting voltage was determined by identifying the intersection of the linear sub-limiting and plateau regions in voltammetry curves. The identification of the limiting voltage of each experiment was further verified by using the measured ohmic resistance (V/I)-voltage curves to identify the voltage at which the resistance of the stack was minimum.

3.3. Transition current measurements

In an ED cell, the formation of CP results in a decrease of current density from its initial non-polarized value down to a stationary current density associated with fully polarized BLs. To determine the impact of the pulsed operation on CP reduction, experiments were carried out to measure the transient current density during the first 60 s of operation once voltage is applied to the stack. The voltage applied during the on periods for both CED and PED was set to 4.5 V, equivalent to 90 % of CED's limiting voltage for a feedwater salinity of 250 mg/L NaCl. Similar to the limiting current measurement tests, feedwater was recirculated at 9 L/h from a 2 L tank. PED parameters varied within a frequency range of 0.5–100 Hz and a duty cycle range of 20–80 %. To enable direct comparisons of current density between the two modes of operation, the cycle-averaged current density, $I_{cyc\text{-}avg}$ (Eq. (23)), is used when comparing PED to CED.

$$I_{cyc-avg} = \frac{t_{On} I_{On} + t_{Off} I_{Off}}{t_{On} + t_{Off}} = \alpha I_{On} \tag{23}$$

3.4. Desalination experiments

Batch desalination experiments were performed to determine the effects of the pulsed operation on desalination time and SEC. The starting and final salinities of the performed batches were 2000 and 250 mg/L NaCl, respectively. Diluate and concentrate streams were recirculated with flowrates of 9 L/h through two separate 500 mL feed tanks. A water recovery ratio of 50 % was set for all the experiments. PED batches were conducted at frequencies of 0.5 and 100 Hz and duty cycles of 20 and 50 %. The input voltages ranged from 4.5 to 9.5 V, selected according to the limiting voltages of CED and PED operated under the conditions detailed above at target salinity. SEC is calculated for these experiments as follows, where V_{batch} is the volume of the batch.

$$SEC = \frac{\int U(t) I(t) dt}{V_{batch}} \tag{24}$$

4. Results and discussion

Concentration drops in the DBL result in decreases in ion transport fluxes through membranes, lowering the generated current density across an ED cell. Implementing pulsed operation allows for boundary concentrations to return back to their bulk values during pauses. Fig. 5a demonstrates the modeling results, detailing the evolution of Na^+ concentration profiles within the CEM and the adjacent DBL and CBL during a pulsing cycle ($t_{on} + t_{off}$) for PED with the frequency of 0.5 Hz and duty cycle of 50 % operated at 90 % of the limiting voltage of the associated CED ($0.9 * U_{lim,CED}$). Due to the electroneutrality assumption, the concentration distributions of Cl^- in BLs are identical to those of Na^+. Inside the CEM, the concentration of Cl^- is calculated by subtracting the fixed charge concentration from that of Na^+. Concentration gradients formed during pulses are sharper at the membrane-solution interface due to the faster transport of ions through IEMs. During pauses, diffusion is the main ion transport mechanism, which promotes concentration recovery in BLs. Once the current density is set to zero, retrieval of the concentration profile begins at the interface due to the existence of a greater driving force for diffusion fluxes (sharper concentration gradients). However, the degree to which CP is reduced depends on the relative duration of the pauses to the time required for ions to diffuse across the BLs. For the system modeled here, the BL thickness is $\delta = 45$ μm and the characteristic time of diffusion of species i is $\tau_{diff} = \delta^2/D_i = 1.5$ s. Hence, a relatively short t_{off} compared to τ_{diff} would prevent the full recovery of uniform concentration profiles in BLs.

Fig. 5b compares the modeling results for current densities of PED (f = 0.5 Hz and α = 50 %) and CED operated under the same voltage ($0.9U_{lim,CED}$) with a feedwater salinity of 4.3 mol/m^3 (250 mg/L) NaCl. At time zero, when the concentration profiles within BLs are still uniform and have yet to polarize, the observed current density is at its maximum. In conventional operation, CP results in a reduction of current density from its initial non-polarized state down to a stationary value which corresponds to the fully polarized BLs. In pulsed operation, attenuating CP throughout pauses leads to higher current density compared to CED in the subsequent on-period, as demonstrated in Fig. 5b.

Despite the higher current density during pulses, the loss of ion transport during pauses results in lower $I_{cyc\text{-}avg}$ compared to the current density of CED, raising the desalination time and energy consumption of PED. Tuning pulsing parameters can improve DR through increasing I_{on} to compensate for zero current density during off periods. Increasing the pulsing voltage, frequency, and duty cycle are viable approaches for enhancing I_{on}. However, the maximum allowable imposed voltage to ED is constrained by limiting conditions, beyond which water dissociation and pH changes become significant. Increasing the frequency and duty cycle may adversely affect the effectiveness of pulsed operation on modulating CP. The energy efficiency of PED is another essential factor

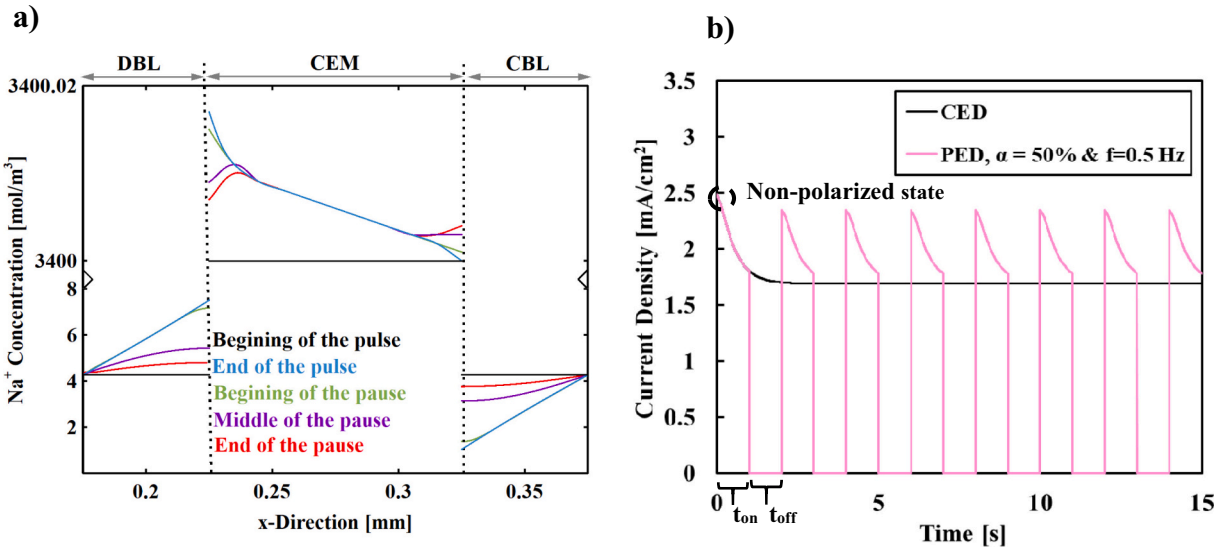

Fig. 5. a) Modeling results of concentration distributions in the diluate and concentrate boundary layers and inside CEM during one pulsing cycle, b) comparison of modeling results for current density versus time in PED and CED. Feedwater salinity = 4.3 mol/m^3 NaCl, U_{pulse} = 0.9 of $U_{lim,CED}$, f = 0.5 Hz, α = 50 %.

that should be taken into account when adjusting pulsing parameters. In the following sections, modeling and experimental results are provided and discussed to illustrate the impacts of pulsing parameters on limiting conditions, pH changes, current density, DR, and SEC of ED.

4.1. Effects of temporal parameters of pulsing on limiting conditions in ED

Limiting condition occurs once ion concentrations at the membrane/solution interface approach zero due to the severe CP in the cell. The limiting voltages for CED and PED (at α = 50 % and f = 100 Hz) with feedwater concentration of 4.3 mol/m^3 NaCl are estimated using the experimentally measured voltammetry curves presented in Fig. 6a. Pulsed operation enhanced the limiting voltage in ED, suggesting that pulsing alleviated the concentration depletion in the DBL and successfully reduced CP formation. Fig. 6b depicts the calculated concentration distributions in the DBL in the vicinity of the CEM for conventional operation at a single cell voltage of 1.5 V compared to the concentration profiles at the end of on periods for pulsed operation at 1.5 and 2.3 V. Note that the voltages used in the model are the potential differences over a single cell pair while the experimental measurements represent the potential drops over the entire ED stack, which contains three cell pairs. The modeling results indicate that under the same cell voltage (1.5 V), the concentration of ions at the membrane/solution interface in PED is higher than that of CED. To approach near zero concentration at the interface and reach the limiting condition, a higher voltage (2.3 V) should be imposed on an ED cell operated under pulsed mode. Preventing the formation of full CP, by cutting the current density and allowing for the concentration recovery to occur in BLs, results in lower concentration depletion in the DBL of PED, increasing the limiting voltage under pulsed operation consistent with experimental observation (Fig. 6a).

Due to the dynamic nature of CP, the limiting conditions in PED vary according to the selected pulsing temporal parameters. Fig. 7a provides a comparison of the experimentally identified limiting voltages of CED and those of PED at duty cycles of 20–80 % and frequencies of 0.5–100 Hz with feedwater salinity of 4.3 mol/m^3. The limiting voltage of PED, $U_{PED,lim}$, increased at lower duty cycles and higher frequencies of pulsing. At a duty cycle of 20 % and a frequency of 100 Hz, the limiting voltage increased by more than two-fold compared to CED. However, the ratio of limiting voltage of PED over CED always remained lower than 1/α, resulting in a cycle-averaged limiting voltage ($\alpha U_{pulse,lim}$) smaller than $U_{CED,lim}$. The higher limiting voltage of PED allows for imposing a voltage greater than U_{CED} during the pulsing periods with an upper bound set by the limiting voltage of PED. Fig. 7b demonstrates the limiting current density of CED, $I_{lim,CED}$, along with the cycle-averaged limiting current density of PED, $I_{lim,PED}$, at duty cycles of 20–80 % and frequencies of 0.5–100 Hz for feedwater salinity of 4.3 mol/m^3. $I_{lim,PED}$ increased by decreasing the duty cycle and increasing the frequency of pulsing due to the higher limiting potential under such conditions. However, $I_{lim,PED}$ was lower than $I_{lim,CED}$ under all pulsing frequencies and duty cycles. These results indicate that for PED operated at limiting and sub-limiting conditions, the increases in current density during pulses were not sufficient to compensate for the lack of ion transport during the pausing periods. At low salinities, if the goal is for PED to match or exceed the current density and consequently the demineralization rate of CED, PED needs to be operated at the over-limiting regime.

The increased limiting voltage with pulsed operation affects the pH variations in ED. Fig. 8 compares the experimentally measured pH of the diluate channel in CED and PED (α = 50 % and f = 100 Hz) with feedwater salinity of 4.3 mol/m^3 NaCl. The concentration depletion in the DBL under limiting conditions promotes the transfer of H_3O^+ and OH^- across the membranes, raising water dissociation and pH changes. In PED, pH variations became dominant at higher input voltages, indicating the greater presence of ions at the membrane-solution interface to prevent H_3O^+ and OH^- transport across the membrane. The delayed pH changes in PED were consistent with the increased limiting voltage in the system, which both resulted from suppressing CP. Hence, it is speculated that the conflicting reported effects of pulsing on pH variations in prior studies [5,6,10,17,22,26] potentially originated from the differences in the operational regimes of CED and PED (sub-limiting in one while over-limiting in the other). For an equal input voltage, PED should result in lower water dissociation due to the lower concentration depletion in the DBL. Once the voltage imposed on PED during the on periods is much greater than that of CED, pH changes may become intensified due to surpassing the limiting voltage during on periods even with a cycle-averaged voltage (αU_{pulse}, where U_{pulse} is the voltage imposed during the on periods) equivalent or smaller than the input voltage of CED (U_{CED}).

4.2. Effects of frequency on current density

Fig. 9a provides a comparison of the experimentally measured transient current density of CED and the transient cycle-averaged

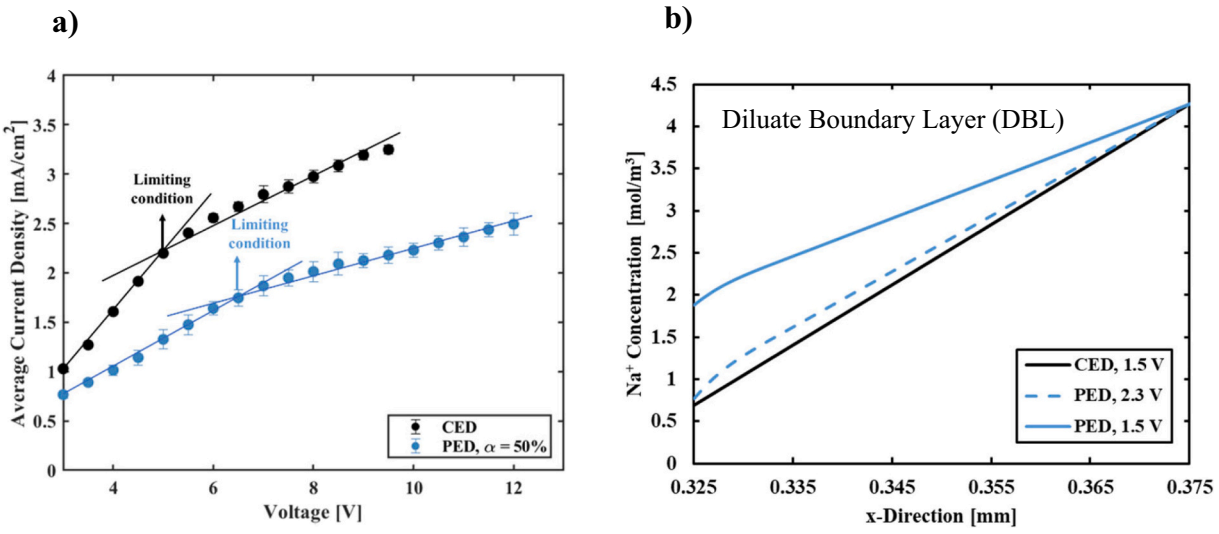

Fig. 6. a) Comparison of the experimentally measured current-voltage curves of CED and PED for feedwater salinity = 4.3 mol/m^3 NaCl, U_{pulse} = 0.9 of $U_{lim,CED}$, f = 100 Hz, and α = 50 %. b) Modeling results for concentration distribution of Na^+ at the end of pulse in diluate boundary layer in the vicinity of the CEM for feedwater salinity of 4.3 mol/m^3: (—) CED at $U_{cell} = U_{lim,CED}$, PED with f = 100 Hz, α = 50 % at $U_{cell} = U_{lim,CED}$ (—) and $U_{cell} = U_{lim,PED}$ (– -).

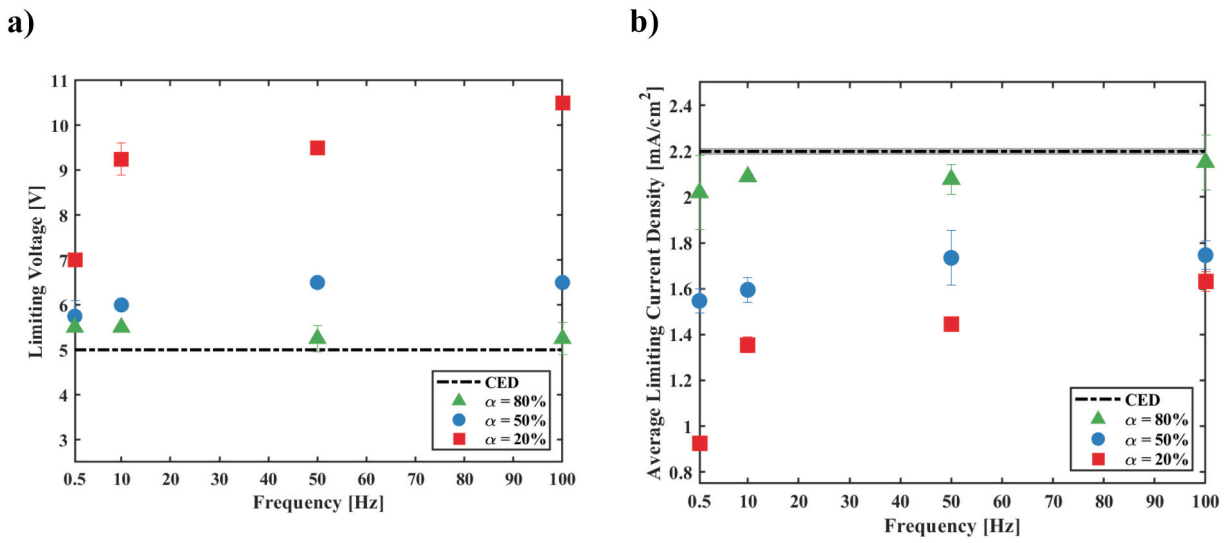

Fig. 7. a) Comparison of the experimentally measured limiting *voltages* in PED and CED, b) comparison of the measured average limiting current densities in PED and CED. Feedwater salinity of 4.3 mol/m^3, (■) α = 20 %, (●) α = 50 %, and (▲) α = 80 %.

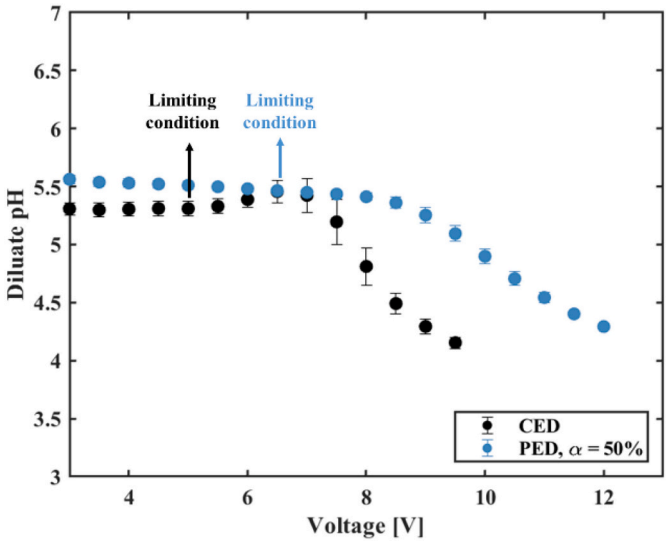

Fig. 8. Comparison of the experimentally measured diluate channel pH in CED and PED for feedwater salinity = 4.3 mol/m^3 NaCl, U_{pulse} = 0.9 of $U_{lim,CED}$, f = 100 Hz, and α = 50 %.

current density of PED at a duty cycle of 50 % and frequencies of 0.5–100 Hz, for feedwater salinity of 4.3 mol/m^3 NaCl and an imposed voltage of 4.5 V ($0.9U_{lim,CED}$). The current density of CED decreased to ~60 % of its initial non-polarized value within 15 s of operation, indicating CP in BLs. In PED, the transition periods were longer (20 s) and the decreases from non-polarized current density were less significant (~20–30 %), specifying the effectiveness of pulsing for reducing CP in the system. Increasing the pulsing frequency from 0.5 to 100 Hz improved the cycle-averaged current density of PED while increasing the deviations between the starting and stationary current density, suggesting a greater CP in the cell.

Above 50 Hz, the growth of current density by frequency was minimal, determining the existence of a threshold beyond which further increases in frequency minimally enhanced current density. As indicated in the figure, the current density of CED reached 98 %, 97 %, and 84 % of its initial non-polarized value within 0.005, 0.01, and 1 s, respectively. Hence, increasing the frequency from 0.5 Hz to 50 Hz (decreasing the on-period from 1 s to 0.01 s) led to a more significant enhancement of current density compared to the increases achieved when changing the frequency from 50 Hz to 100 Hz (decreasing the on-period from 0.01 s to 0.005 s). Moreover, at high frequencies, the pausing period was too brief to allow for significant concentration recovery in BLs. These analyses suggested that the saturation in current density by frequency occurred due to the reduction in the period of a cycle which minimized the extent of CP formation during the on-times and concentration recovery during the off-periods. Similar saturation of current density with frequency was reported previously [12]. Overall, the impacts of pulsing frequency on the current density of PED were marginal when all other variables including the duty cycle were fixed.

Investigating the modeling results of concentration distributions in the DBL helped explain the trends observed in experimental data. Fig. 9b presents the calculated concentration distributions at the end of the transition time in the DBL in the vicinity of the CEM for CED along with those of PED at a duty cycle of 50 % and frequencies of 0.5 and 100 Hz for feedwater salinity of 4.3 mol/m^3 NaCl and an imposed voltage of $0.9U_{lim,CED}$. At the frequency of 0.5 Hz, the concentration distribution at the end of the pulsing period approaches that of CED due to the relatively long pulse time (1 s) which allows for CP to fully form in the BLs. On the other hand, the high duration of the pausing period (1 s) provides the required time for returning the concentration profile in the DBL close to the bulk value. While pulsing at 0.5 Hz enables significant concentration profile relaxation during pauses, full concentration recovery demands even lower frequencies to further increase the pausing periods closer to the characteristic time of diffusion (τ_{diff} = 1.5 s for the system tested). At high frequencies, concentration drops are minimal throughout pulses due to the short duration of the on-time (t_{on}).

Increasing the frequency up to 100 Hz (t_{on} = *0.005* s) reduces the available time for ion transport through the membrane down to 0.05 s, resulting in lower concentration depletion in DBL at the end of the pulsing period compared to those of CED and PED with the frequency of 0.5 Hz. However, concentration recovery only occurs within a narrow region close to the membrane interface due to the short pausing period (0.05 s) at 100 Hz relative to the characteristic time of diffusion (τ_{diff}). At high frequencies, the concentrations in most parts of BLs remain stationary throughout both pulses and pauses, dividing the concentration profiles into the pulsing and stationary regions. However, this stationary concentration is still higher than the concentration reached in CED, determining the effectiveness of the pulsed operation in suppressing CP. The concentration profile in the stationary region of BLs corresponds to the cycle-averaged current density of PED. At low frequencies, pulsed

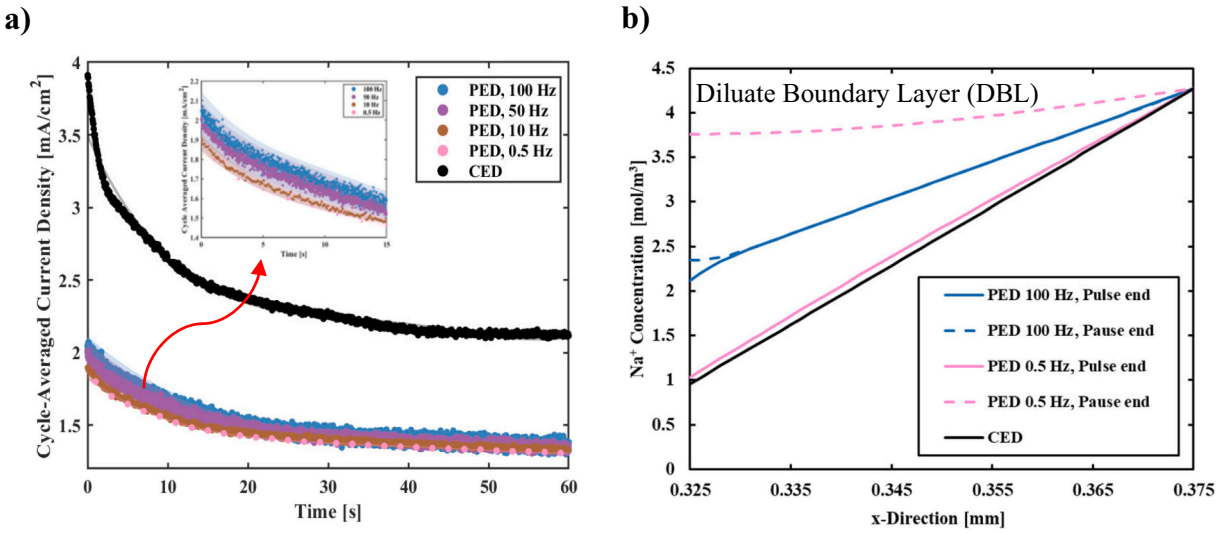

Fig. 9. a) Experimentally measured cycle-averaged current density versus time for PED at α = 50 % and frequencies from 0.5 to 100 Hz compared to current density of CED, b) modeling results for concentration distribution of Na^+ in the diluate boundary layer at the CEM-solution interface at the end of the pulse and pause for PED with α = 50 % and frequencies of 0.5 and 100 Hz compared to concentration distribution for CED. In both figures, feedwater salinity is 4.3 mol/m^3 NaCl and $U_{pulse} = U_{CED} = 0.9$ of $U_{lim,CED}$.

operation improves the performance of ED by providing significant concentration recovery in BLs during pauses while at high frequencies, the benefits gained from pulsing are due to decreasing concentration depletion in BLs during the on-periods.

4.3. Effects of duty cycle on current density

The duty cycle of pulsing affects the current density and desalination rate of PED. Fig. 10a demonstrates the experimentally measured current density of CED compared to the cycle-averaged current density of PED at duty cycles of 20 %, 50 %, and 80 %, and the frequency of 100 Hz for feedwater salinity of 4.27 mol/m^3 NaCl and an imposed voltage of 4.5 V ($0.9U_{lim,CED}$). The cycle-averaged current density of PED increased at higher duty cycles due to the decreases in the duration of pausing periods through which the desalination process was stalled. Fig. 10b demonstrates the calculated concentration distributions at the end of the transition time in the DBL in the vicinity of the CEM for CED and PED with duty cycles of 20 % and 80 % and a frequency of 100 Hz. The concentration distribution in DBL of PED at the end of the pulsing period with the duty cycle of 20 % is significantly higher than that of CED, while the duty cycle of 80 % results in a concentration distribution similar to that of CED.

The improvement of the cycle-averaged current density of PED at high-duty cycles is accompanied by increasing the concentration drops in the DBL during the on-periods, decreasing the effectiveness of the pulsed operation for alleviating CP. Lowering the duty cycle reduced the available time for CP to evolve during pulses, resulting in greater concentrations and lower CP in BLs. At high frequencies, decreasing the duty cycle has a negligible impact on the extent of concentration recovery during the pausing period due to the overall brief cycle time, resulting in pausing durations that are substantially lower than the characteristic time of diffusion (t_{off} = 0.002 s and 0.008 s for duty cycles of 80 % and 20 %, respectively, at 100 Hz, compared to τ_{diff} = 1.5 s). The extent of concentration recovery during the off-periods is mainly

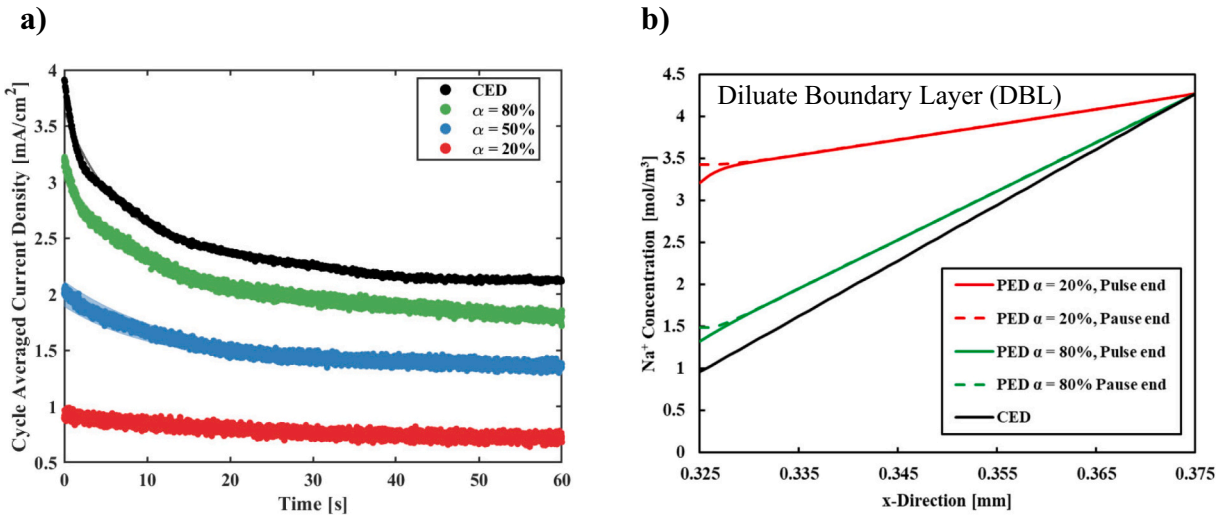

Fig. 10. a) Experimentally measured cycle-averaged current density of PED at 100 Hz and duty cycles from 20 % to 80 % compared to the current density of CED, b) modeling results for concentration distribution of Na^+ in the diluate boundary layer at the CEM-solution interface for PED at 100 Hz and duty cycles of 20 % and 80 % at end of the pulsing compared to concentration distribution of CED. In both figures, feedwater salinity is 4.27 mol/m^3 NaCl and $U_{pulse} = 0.9U_{lim,CED}$.

influenced by the frequency of pulsing rather than the duty cycle. Overall, pulsing parameters should be selected according to the intended objective of the pulsed operation and the chemistry of the feedwater. For scale mitigation purposes where suppressing CP is the main target, lower duty cycles could be preferable despite the reduced current density and desalination rate.

4.4. Effects of pulsing parameters on specific energy consumption and desalination time

The effects of pulsing parameters on concentration distributions and current density significantly influence the time and energy consumption of a desalination batch. Fig. 11a depicts the experimentally measured normalized SEC and batch time of PED at duty cycles of 20 % and 50 %, frequencies of 0.5 and 100 Hz, and pulsing voltages of 4.5, 5.5, and 9.5 V for desalination of 500 mL feedwater from 2000 to 250 mg/L NaCl at water recovery ratio of 50 %. To enable the direct comparison of the effects of varying pulsing parameters, the measured SEC and batch time of PED for desalination of aqueous NaCl solution from 2000 to 250 mg/L are normalized with respect to those of CED at an imposed voltage of 4.5 V ($0.9U_{lim,CED}$). The CED batch time and SEC used for normalization were 43.3 ± 1 % min and 4.33 kWh/m^3 ± 2 %.

As demonstrated in Fig. 11a, PED operation at a frequency of 100 Hz, pulsing voltage of 4.5 V, and duty cycles of 50 % and 20 % led to, respectively, 60 % and 300 % increases in the desalination time compared to CED. Such results indicate that turning off the electric field for (1-α)% of the desalination cycle resulted in less than ($\frac{1-\alpha}{\alpha}$)% increase in the batch time. As discussed earlier, current density during the on-period of PED was greater than that of CED due to decreases of CP in BLs, which reduced the local electrical resistance. The higher current density throughout the on-time partially compensated for the lack of ion transport during the off periods, resulting in a cycle-averaged current density (αI_{on}) that was greater than (αI_{CED}). Therefore, the increases in desalination time remained less than the total off-periods of the batch. Pulsing at higher duty cycles can minimize the increases in the desalination time of PED and improve the feasibility of the approach for brackish water treatment.

For PED and CED batches with the same input voltages, the deviation in SEC of the two operational modes was negligible. Fig. 11b demonstrates the experimentally measured cycle-averaged current density of PED with duty cycles of 20 % and 50 %, a frequency of 100 Hz, and a pulsing voltage of 4.5 V during batch desalination of 500 mL feedwater from 2000 to 250 mg/L NaCl at a water recovery ratio of 50 % compared to the current density of CED at a voltage of 4.5 V. As the batch progressed, current density decreased due to ion transport to the concentrate compartment and CP formation, which resulted in increases in the bulk and BLs resistances in the diluate channel. However, the initial and final current densities of PED for the same feed and product water salinities were greater than αI_{CED}, indicating the effectiveness of the pulsed operation in successfully reducing CP and lowering the increases in boundary resistances. Such impact could enhance the energy efficiency of the approach compared to CED due to the reduction in energy dissipation in BLs. However, the increases in batch time due to the pausing periods offset the energy-saving gains achieved by suppressing CP, resulting in normalized SEC close to unity as indicated in Fig. 11a. At a duty cycle of 50 %, a frequency of 100 Hz, and a pulsing voltage of 4.5 V, the less significant increase in the batch time resulted in a slightly lower SEC for PED compared to CED due to lower inefficiencies and boundary resistances with the pulsed operation.

As discussed earlier, increasing the frequency and voltage of pulsing enhanced the cycle-averaged current density of PED, increasing ion transport from diluate to concentrate compartments. Fig. 11a demonstrates that increasing the frequency from 0.5 to 100 Hz led to decreases in the batch time and SEC of PED with a duty cycle of 50 % and a pulsing voltage of 4.5 V. Due to the marginal impacts of frequency on cycle-averaged current density, the decreases in SEC and desalination time were relatively minor as well. At a duty cycle of 50 % and a frequency of 100 Hz, increasing the pulsing voltage up to 5.5 V (0.9 * $U_{lim,PED}$) resulted in a 40 % decrease in desalination time and an approximately 20 % additional energy consumption compared to PED operated at 4.5 V. Such results suggest that under the same duty cycle and frequency, increasing the imposed voltage during the on-time close to the limiting value of PED could enhance the desalination rate but increases the SEC of the process due to the higher input voltage. Increasing the pulsing voltage from 4.5 (0.9 * $U_{lim,CED}$) to 9.5 V (0.9 * $U_{lim,PED}$) in PED with the frequency of 100 Hz and duty cycle of 20 % intensified the SEC of the process two-fold while resulting in a four times decrease in desalination time. Under this condition, the energy saved from the reduced desalination time could not totally compensate for the energy consumption increase due to the higher input voltage. Once the imposed pulsing

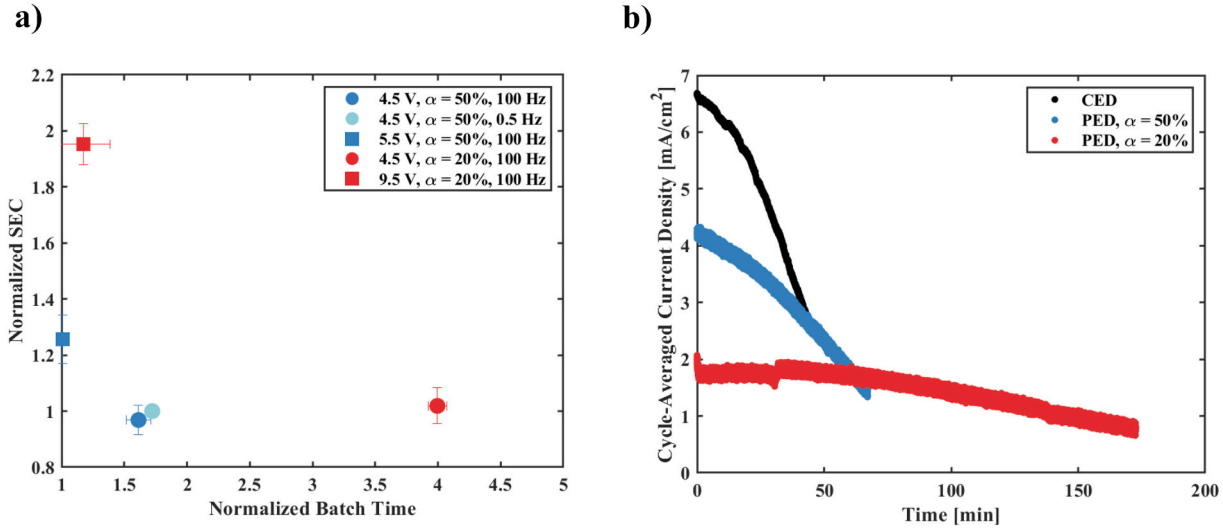

Fig. 11. a) Experimentally measured normalized SEC versus normalized batch time. f = 100 Hz, α = 50 %, U_{pulse} = 0.9 * $U_{lim,CED}$ = 4.5 V (●); f = 0.5 Hz, α = 50 %, U_{pulse} = 0.9 * $U_{lim,CED}$ = 4.5 V (●); f = 100 Hz, α = 50 %, U_{pulse} = 0.9 * $U_{lim,PED}$ = 5.5 V (■); f = 100 Hz, α = 20 %, U_{pulse} = 0.9 * $U_{lim,CED}$ = 4.5 V (●); f = 100 Hz, α = 20 %, U_{pulse} = 0.9 * $U_{lim,PED}$ = 9.5 V (■), b) cycle-averaged current density versus the batch time for f = 100 Hz, α = 50 %, U_{pulse} = 0.9 * $U_{lim,CED}$ = 4.5 V (●); f = 100 Hz, α = 20 %, U_{pulse} = 0.9 * $U_{lim,CED}$ = 4.5 V (●) compared to current density of CED (●). The batch experiments are conducted for desalination of 500 mL of feedwater from 2000 to 250 mg/L NaCl at water recovery ratio of 50 %.

voltage is $U_{lim,PED}$, the boundary concentration profiles during the on-period approach that of CED operated at $U_{lim,CED}$ (Fig. 6b). Hence, increasing the voltage decreases the effectiveness of pulsing for CP reduction in the BLs while increasing the SEC relative to CED as well.

For scale mitigation purposes in which reducing CP is the main objective of pulsed operation, imposing the same voltage as that of CED is more appropriate even though it reduces the desalination rate. The extent of CP formation in channels is affected by the salinity and composition of the feedwater, ED stack size, and channel velocity. To be truly effective, pulsing parameters should be tuned according to the specific water type, system size, and operational conditions. In addition to the consideration regarding the energy consumption and desalination time, the type of existing scale-forming components and their selective transport across the membranes should be taken into account in optimizing the pulsing parameters. The parametric understanding gained in this study provides the foundation required for the development of a generalizable optimization scheme that can be applied to various desalination scenarios.

5. Conclusions

In this study, the effects of pulsed operation of ED on the desalination performance and energy consumption of the process were thoroughly investigated. A facile 1-D ion transport model was developed to evaluate the concentration distributions in the cell, which were experimentally cumbersome to identify. The limiting condition, pH changes, transition current, batch time, and SEC were measured for conventional and pulsed ED to provide a comprehensive assessment of the impacts of the pulsing with various parameters on the desalination performance of the system.

The results indicated that pulsing postponed the limiting conditions in ED, increasing the voltage at which pH variations were significant. Due to the dynamic nature of CP, the degree of increase in limiting voltage depended on the pulsing frequency and duty cycle. However, the cycle-averaged limiting current densities of PED were lower than those of CED over the entire range of examined t_{on}/t_{off} ratios. These results emphasize that for galvanostatic operation, care must be taken to avoid setting the current density of PED according to the limiting current density of CED since it may result in over-limiting conditions and increased pH changes in PED. Furthermore, increasing the frequency of pulsing up to a threshold improved the current density and desalination rate of the process. Higher duty cycles and pulsing voltage also led to greater current densities in the system, however, reduced the effectiveness of the approach for moderating concentration polarization. Under an equal input voltage, the pulsed operation lowered the desalination rate compared to CED but resulted in approximately similar SEC.

The results of this study elucidate the effects of pulsing parameters on the desalination performance of ED and shed light on the existing knowledge gap on various aspects of the process. These conclusions are necessary considerations when optimizing pulsed operation as an energy-efficient and cost-effective scale mitigation strategy. While the evaluation of scale mitigation benefits should be conducted with feed water containing scale-forming components, the results of this study with non-scaling feedwater provide the guideline required to narrow down the effective range of the pulsing parameters to preserve the scale mitigation benefits of PED while avoiding a significant reduction in the desalination rate. Even though low-duty cycles mitigate concentration polarization more efficiently, the losses in the desalination rate under such low-duty cycles significantly reduce the feasibility of the approach due to the increased pumping energy. Inputting voltages greater than U_{CED} enhances the production rate but decreases the effectiveness of pulsing in modulating concentration polarization and increases the SEC significantly, reducing the viability of the approach as a scale mitigation strategy. According to these results, a duty cycle of 50 % and a pulsing voltage same as U_{CED} will make the desalination rate and SEC of PED within reasonable ranges and improve the viability of pulsing for scale mitigation. Under a fixed duty cycle, the t_{on} to t_{off} ratio in PED should be adjusted by tuning the frequency of pulsing based on the ratio of the scaling and non-scaling components in the feedwater to control the transport rate of scale-forming species to the concentrate channel.

CRediT authorship contribution statement

S. Honarparvar: Investigation, acquisition of data, analysis and/or interpretation of data, development of the modeling framework, writing - the original draft, writing - review & editing.

R. Al-Rashed: Investigation, acquisition of data, analysis and/or interpretation of data, writing - the original draft, writing - review & editing.

A. G. Winter: Conceptualization and design of the study, funding acquisition, project administration, resources, supervision, revising the manuscript for important intellectual content.

Declaration of competing interest

The authors declare that they have no known competing financial interests or personal relationships that could have appeared to influence the work reported in this paper.

Data availability

All the data used in this article are provided in the manuscript

Acknowledgments

This work was sponsored by the United States Bureau of Reclamation Desalination and Water Purification Research and Development Program grant R19AC00104, and Kuwait University.

References

[1] J.S. Stanton, D.W. Anning, C.J. Brown, R.B. Moore, V.L. McGuire, S.L. Qi, A. C. Harris, K.F. Dennehy, P.B. McMahon, J.R. Degnan, Brackish Groundwater in the United States; 2330-7102, US Geological Survey, 2017.
[2] IDA, The 19th IDA Worldwide Desalting Plant Inventory, 2006.
[3] S.K. Patel, M. Qin, W.S. Walker, M. Elimelech, Energy efficiency of electro-driven brackish water desalination: electrodialysis significantly outperforms membrane capacitive deionization, Environ. Sci. Technol. 54 (2020) 3663–3677.
[4] S.K. Patel, P.M. Biesheuvel, M. Elimelech, Energy consumption of brackish water desalination: identifying the sweet spots for electrodialysis and reverse osmosis, ACS ES&TEngineering 1 (2021) 851–864.
[5] N. Mishchuk, S. Verbich, F. Gonzales-Caballero, Concentration polarization and specific selectivity of membranes in pulse mode, Colloid J. 63 (2001) 586–595.
[6] C. Casademont, P. Sistat, B. Ruiz, G. Pourcelly, L. Bazinet, Electrodialysis of model salt solution containing whey proteins: enhancement by pulsed electric field and modified cell configuration, J. Membr. Sci. 328 (2009) 238–245.
[7] N. Cifuentes-Araya, G. Pourcelly, L. Bazinet, Impact of pulsed electric field on electrodialysis process performance and membrane fouling during consecutive demineralization of a model salt solution containing a high magnesium/calcium ratio, J. Colloid Interface Sci. 361 (2011) 79–89.
[8] N. Cifuentes-Araya, G. Pourcelly, L. Bazinet, Water splitting proton-barriers for mineral membrane fouling control and their optimization by accurate pulsed modes of electrodialysis, J. Membr. Sci. 447 (2013) 433–441.
[9] N. Lemay, S. Mikhaylin, S. Mareev, N. Pismenskaya, V. Nikonenko, L. Bazinet, How demineralization duration by electrodialysis under high frequency pulsed electric field can be the same as in continuous current condition and that for better performances? J. Membr. Sci. 117878 (2020).
[10] S. Mikhaylin, V. Nikonenko, G. Pourcelly, L. Bazinet, Intensification of demineralization process and decrease in scaling by application of pulsed electric field with short pulse/pause conditions, J. Membr. Sci. 468 (2014) 389–399.
[11] N. Lemay, S. Mikhaylin, L. Bazinet, Voltage spike and electroconvective vortices generation during electrodialysis under pulsed electric field: Impact on demineralization process efficiency and energy consumption, Innovative Food Sci. Emerg. Technol. 52 (2019) 221–231.
[12] P. Sistat, P. Huguet, B. Ruiz, G. Pourcelly, S. Mareev, V. Nikonenko, Effect of pulsed electric field on electrodialysis of a NaCl solution in sub-limiting current regime, Electrochim. Acta 164 (2015) 267–280.
[13] D. Butylskii, I. Moroz, K. Tsygurina, S. Mareev, Effect of surface inhomogeneity of ion-exchange membranes on the mass transfer efficiency in pulsed electric field modes, Membranes 10 (2020) 40.
[14] M. Andreeva, V. Gil, N. Pismenskaya, L. Dammak, N. Kononenko, C. Larchet, D. Grande, V. Nikonenko, Mitigation of membrane scaling in electrodialysis by

electroconvection enhancement, pH adjustment and pulsed electric field application, J. Membr. Sci. 549 (2018) 129–140.
[15] S. Suwal, J. Amiot, L. Beaulieu, L. Bazinet, Effect of pulsed electric field and polarity reversal on peptide/amino acid migration, selectivity and fouling mitigation, J. Membr. Sci. 510 (2016) 405–416.
[16] A. Merkel, A.M. Ashrafi, An investigation on the application of pulsed electrodialysis reversal in whey desalination, Int. J. Mol. Sci. 2019 (1918) 20.
[17] P. Malek, J. Ortiz, B.S. Richards, A.I. Schaefer, Electrodialytic removal of NaCl from water: Impacts of using pulsed electric potential on ion transport and water dissociation phenomena, J. Membr. Sci. 435 (2013) 99–109.
[18] H.-J. Lee, J.-S. Park, S.-H. Moon, A study on fouling mitigation using pulsing electric fields in electrodialysis of lactate containing BSA, Korean J. Chem. Eng. 19 (2002) 880–887.
[19] H.-J. Lee, S.-H. Moon, S.-P. Tsai, Effects of pulsed electric fields on membrane fouling in electrodialysis of NaCl solution containing humate, Sep. Purif. Technol. 27 (2002) 89–95.
[20] H.-J. Lee, S.-J. Oh, S.-H. Moon, Recovery of ammonium sulfate from fermentation waste by electrodialysis, Water Res. 37 (2003) 1091–1099.
[21] H.-J. Lee, S.-H. Moon, Enhancement of electrodialysis performances using pulsing electric fields during extended period operation, J. Colloid Interface Sci. 287 (2005) 597–603.
[22] B. Ruiz, P. Sistat, P. Huguet, G. Pourcelly, M. Araya-Farias, L. Bazinet, Application of relaxation periods during electrodialysis of a casein solution: impact on anion-exchange membrane fouling, J. Membr. Sci. 287 (2007) 41–50.
[23] N. Mishchuk, L. Koopal, F. Gonzalez-Caballero, Intensification of electrodialysis by applying a non-stationary electric field, Colloids Surf. A Physicochem. Eng. Asp. 176 (2001) 195–212.
[24] N. Cifuentes-Araya, G. Pourcelly, L. Bazinet, How pulse modes affect proton-barriers and anion-exchange membrane mineral fouling during consecutive electrodialysis treatments, J. Colloid Interface Sci. 392 (2013) 396–406.
[25] N. Cifuentes-Araya, G. Pourcelly, L. Bazinet, Multistep mineral fouling growth on a cation-exchange membrane ruled by gradual sieving effects of magnesium and carbonate ions and its delay by pulsed modes of electrodialysis, J. Colloid Interface Sci. 372 (2012) 217–230.
[26] P. Sosa-Fernandez, J. Post, M. Ramdlan, F. Leermakers, H. Bruning, H. Rijnaarts, Improving the performance of polymer-flooding produced water electrodialysis through the application of pulsed electric field, Desalination 484 (2020), 114424.
[27] G. Dufton, S. Mikhaylin, S. Gaaloul, L. Bazinet, Positive impact of pulsed electric field on lactic acid removal, demineralization and membrane scaling during acid whey electrodialysis, Int. J. Mol. Sci. 20 (2019) 797.
[28] E. Jones, M. Qadir, M.T. van Vliet, V. Smakhtin, S.-M. Kang, The state of desalination and brine production: a global outlook, Sci. Total Environ. 657 (2019) 1343–1356.
[29] M.C. Martí-Calatayud, M. Sancho-Cirer Poczatek, V. Pérez-Herranz, Trade-off between operating time and energy consumption in pulsed electric field electrodialysis: a comprehensive simulation study, Membranes 11 (2021) 43.
[30] N. Mishchuk, Perspectives of the electrodialysis intensification, Desalination 117 (1998) 283–295.
[31] Y. Kim, W.S. Walker, D.F. Lawler, Electrodialysis with spacers: effects of variation and correlation of boundary layer thickness, Desalination 274 (2011) 54–63.
[32] S. Honarparvar, C.C. Chen, D. Reible, Modeling ion transport in electrodialysis of concentrated solutions, in: Advances In Water Desalination Technologies, 2021, pp. 193–226.
[33] R. Kingsbury, S. Zhu, S. Flotron, O. Coronell, Microstructure determines water and salt permeation in commercial ion-exchange membranes, ACS Appl. Mater. Interfaces 10 (2018) 39745–39756.
[34] M. Tedesco, H. Hamelers, P. Biesheuvel, Nernst-Planck transport theory for (reverse) electrodialysis: II. Effect of water transport through ion-exchange membranes, J. Membr. Sci. 531 (2017) 172–182.
[35] M.A.-K. Urtenov, E.V. Kirillova, N.M. Seidova, V.V. Nikonenko, Decoupling of the Nernst– Planck and Poisson equations. application to a membrane system at overlimiting currents, J. Phys. Chem. B 111 (2007) 14208–14222.
[36] J. Mackie, P. Meares, The diffusion of electrolytes in a cation-exchange resin membrane I. Theoretical, Proceedings of the Royal Society of London. Series A. Mathematical and Physical Sciences 232 (1955) 498–509.
[37] T. Scarazzato, D.C. Buzzi, A.M. Bernardes, J.A.S. Tenório, D.C.R. Espinosa, Current-voltage curves for treating effluent containing HEDP: determination of the limiting current, Braz. J. Chem. Eng. 32 (2015) 831–836.